doi:10.1016/j.jmb.2009.03.077 *J. Mol. Biol.* (2009) **xx**, xxx–xxx

JMB

Available online at www.sciencedirect.com

ScienceDirect

ELSEVIER

The Crystal Structure of UehA in Complex with Ectoine—A Comparison with Other TRAP-T Binding Proteins

Justin Lecher[1]†, Marco Pittelkow[2]†, Silke Zobel[1], Jan Bursy[2], Tobias Bönig[2], Sander H.J. Smits[1], Lutz Schmitt[1]* and Erhard Bremer[2]

[1]*Institute of Biochemistry, Heinrich-Heine-University Duesseldorf, Universitätsstrasse 1, 40225 Duesseldorf, Germany*

[2]*Laboratory for Microbiology, Department of Biology, Philipps University Marburg, Karl-von-Frisch Strasse 8, D-35032 Marburg, Germany*

Received 20 February 2009; received in revised form 30 March 2009; accepted 31 March 2009

Edited by R. Huber

Substrate-binding proteins or extracellular solute receptors (ESRs) are components of both ABC (ATP binding cassette) and TRAP-T (tripartite ATP-independent periplasmic transporter). The TRAP-T system UehABC from *Silicibacter pomeroyi* DSS-3 imports the compatible solutes ectoine and 5-hydroxyectoine as nutrients. UehA, the ESR of the UehABC operon, binds both ectoine and 5-hydroxyectoine with high affinity (K_d values of 1.4±0.1 and 1.1±0.1 μM, respectively) and delivers them to the TRAP-T complex. The crystal structure of UehA in complex with ectoine was determined at 2.9-Å resolution and revealed an overall fold common for all ESR proteins from TRAP systems determined so far. A comparison of the recently described structure of TeaA from *Halomonas elongata* and an ectoine-binding protein (EhuB) from an ABC transporter revealed a conserved ligand binding mode that involves both directed and cation–pi interactions. Furthermore, a comparison with other known TRAP-T ESRs revealed a helix that might act as a selectivity filter imposing restraints on the ESRs that fine-tune ligand recognition and binding and finally might determine the selection of the cognate substrate.

Keywords: TRAP transporters; periplasmic binding proteins; ectoine; compatible solutes

Introduction

Effective transport systems are required for the survival and growth of microorganisms in their natural habitats to permit scavenging of nutrients, ions and osmolytes. Some of these transporters, such as the ATP binding cassette (ABC) transport systems, require a substrate-binding protein (SBP), also known as extracellular solute receptor (ESR), to catalyze ATP-driven substrate uptake.[1,2] In such binding protein-dependent ABC transporters, initial recognition of the ligand is accomplished with high affinity and specificity by the SBP that is either located in the periplasm of Gram-negative bacteria or anchored at the cell surface of Gram-positive bacteria or archaea.[1] After initial ligand binding, the substrate-loaded SBP delivers the ligand to the designated membrane-embedded components of the ABC transporter for subsequent ATP-dependent import. The SBP is essential for substrate uptake, imposes directionality on a given ABC transporter and regulates the ATPase activity of the nucleotide-binding protein.[3]

In a pioneering study, Forward *et al.*[4] identified a novel multicomponent transport system in the photosynthetic bacterium *Rhodobacter capsulatus* that contained an ESR, but this transport system, in striking contrast to ABC transporters, operated independently of ATP hydrolysis. These transporters were subsequently named TRAP-Ts (tripartite ATP-independent periplasmic transporters),[5] and they use electrochemical ion gradients (H^+ or Na^+) to fuel the uphill transport of substrates. TRAP systems are thus secondary active transporters but require an ESR for proper functioning.[6–9] In the

*Corresponding author. E-mail address: lutz.schmitt@uni-duesseldorf.de.

† J.L. and M.P. contributed equally to this work.

Abbreviations used: ESR, extracellular solute receptor; ABC, ATP binding cassette; TRAP-T, tripartite ATP-independent periplasmic transporter; SBP, substrate-binding protein; Usp, universal stress protein.

0022-2836/$ - see front matter © 2009 Published by Elsevier Ltd.

following, we use the term "SBP" for the binding proteins of ABC transport systems and the term "ESR" for the binding protein of TRAP-Ts to differentiate between both families.

Systematic genome-wide bioinformatic analysis revealed a widespread distribution of TRAP-Ts within the domains of bacteria and archaea, with an increased number of TRAP-type transporters found in microorganisms living in saline environments.[8] Use of electrochemical sodium gradients to energize TRAP-Ts would be advantageous to marine microorganisms because it would allow these bacteria to import substrates at a lower energetic cost than that required for the functioning of an ABC transporter uptake system that depends on ATP hydrolysis.[8] *In vitro* reconstitution of the sialic acid-specific SiaPQM system from the human pathogen *Haemophilus influenzae* demonstrated that a sodium gradient is used to fuel substrate import by a TRAP-type system.[9]

TRAP-Ts, as exemplified by the C4-dicarboxylate import system (DctPQM) from *R. capsulatus*,[4,5] usually comprise three components: a large membrane-embedded subunit (DctM), a small membrane-embedded subunit (DctQ) and an extracellular SBP (DctP), the ESR. The large subunit probably forms the solute translocation channel[7,8] and usually comprises 12 transmembrane-spanning segments. The small subunit contains 4 transmembrane-spanning segments. Both proteins are required for the functioning of the TRAP-T, but the precise role of the single subunits in the overall transport process is still unclear[7,8] In some TRAP systems, such as SiaPQM, the large and small membrane subunits are fused in a single polypeptide.[9] The best studied components of TRAP systems are the soluble ESRs.[10–16] *In vitro* studies with the SiaPQM system have recently shown that the SBP imposes directionality on the overall transport process,[9] but it is so far unclear whether the observed binding protein-dependent export reaction of a TRAP system is of physiological relevance.

Several ESR crystal structures, with or without bound ligand, have advanced our understanding of the ESR proteins of TRAP systems. These crystal structures include SiaP from *H. influenzae*,[12,17] specific for sialic acids; TakP from *Rhodobacter sphaeroides*,[13] specific for α-keto acids; DctP6 and DctP7 from *Bordetella pertussis*,[14] both specific for pyroglutamic acid; TeaA from *Halomonas elongata*,[15] specific for ectoine and 5-hydroxyectoine; and the structure of an ESR from the hyperthermophile *Thermotoga maritima*,[16] with a serendipitously captured and chemically poor defined substrate. Structural analysis of these ESRs revealed a common protein fold and the same bilobal organization observed for SBPs.[18,19] Furthermore, the structural analysis of the SiaP and TakP proteins in the presence and in the absence of their specific ligands suggested that both proteins follow the "Venus flytrap" mechanism of SBPs for capturing of the cognate ligand.[12,13,19] This mechanism proposes a constant opening-and-closing motion of the bilobal SBPs of ABC transporters. The binding of the ligand shifts the equilibrium between these various conformations toward the closed state in which the substrate has been trapped by the SBP.[18] A flexible linker connects the two domains of the SBP and permits a hinge-bending movement that leads to rigid-body motions conducted by both domains of the SBP. As a consequence, the ligand-binding site is dynamically formed with contributions of both domains of the SBP and, concomitantly, the ligand is trapped within the deep cleft formed by the two domains of the SBP. The structural investigations support the idea that the TRAP-associated ESRs and ABC-associated SBPs are functionally similar with respect to their role in transport.[8,12,17]

In this study, we focused on the ectoine/5-hydroxyectoine ligand-binding protein UehA from *Silicibacter pomeroyi* DSS-3,[20] a member of the *Roseobacter* lineage of marine α-proteobacteria that plays an important role for global carbon and sulfur cycles in oceans.[21] *S. pomeroyi* DSS-3 possesses an uncommonly high number of TRAP transport systems,[8] one of which is the UehABC importer. Herein, we show that ectoine and 5-hydroxyectoine are two natural ligands of UehA. Both ligands are compatible solutes that are widely used by microorganisms to offset the detrimental effects of high salinity on cell physiology.[22] However, *S. pomeroyi* DSS-3 does not use these tetrahydropyrimidines as osmoprotectants and instead employs them as nutrients.

We determined the crystal structure of the UehA–ectoine complex and compared the overall fold of UehA and the architecture of the ligand-binding site with those of the TeaA–ectoine complex.[15] TeaA is an ESR from an ectoine/5-hydroxyectoine-specific TRAP-T involved in osmoprotection in the moderate halophile *H. elongata*.[23] Furthermore, we compared the UehA–ectoine complex with the crystal structure of an ectoine and 5-hydroxyectoine-specific SBP (EhuB).[24] Finally, a comparison of all available crystal structures of ESRs from TRAP systems revealed a helix within these ligand-binding proteins that probably plays an important role in fine-tuning and determining the substrate selectivity of TRAP-associated ESRs.

Results and Discussion

A putative TRAP-T for ectoine and 5-hydroxyectoine in *S. pomeroyi* DSS-3

In marine waters, the nutrient concentrations are generally low and microorganisms must therefore possess effective mechanisms to scavenge organic compounds from such an oligotrophic environment. The marine bacterium *S. pomeroyi* DSS-3 is a member of the ecologically important *Roseobacter* lineage of α-proteobacteria,[21] and its genome sequence has revealed a number of adaptations to nutrient-poor environments. Among these is the occurrence of an

Please cite this article as: Lecher, J. *et al.*, The Crystal Structure of UehA in Complex with Ectoine—A Comparison with Other TRAP-T Binding Proteins, *J. Mol. Biol.* (2009), doi:10.1016/j.jmb.2009.03.077

uncommonly large number of TRAP-Ts.[8,20] We found that *S. pomeroyi* DSS-3 can efficiently use the tetrahydropyrimidines ectoine and 5-hydroxyectoine (see Fig. 3 for their chemical structures) as sole nitrogen and carbon sources. Hence, an uptake system for ectoine and 5-hydroxyectoine must operate in *S. pomeroyi* DSS-3 to provide the cell with these compounds as nutrients. Surprisingly, both compatible solutes did not function as osmostress protectants in *S. pomeroyi* DSS-3 (J.B., T.B. and E.B., unpublished results) as they commonly do in many bacterial species.[22,25–28]

Inspection of the *S. pomeroyi* DSS-3 genome sequence[20] identified a large gene cluster (Fig. 1a) whose predicted proteins encode a TRAP-type import system for ectoine and 5-hydroxyectoine and enzymes mediating the degradation of these compounds for nutritional purposes. The components of the TRAP-type transporter UehABC (Ueh: *u*ptake of *e*ctoine and *h*ydroxyectoine) are related to the subunits of a functionally characterized ectoine/5-hydroxyectoine TRAP transport system (TeaABC) from the moderate halophile *H. elongata*.[23] The TeaABC system serves for the osmotically regulated import of ectoine and 5-hydroxyectoine as osmoprotectants and as a salvaging system for ectoine/5-hydroxyectoine that leaks from the ectoine/5-hydroxyectoine-producing *H. elongata* cells.[23] Genes encoded downstream of *uehABC* are referred to as *eutABCDE* (Eut: *e*ctoine *ut*ilization) and *spo1137*/*spo1136* (Fig. 1a). The EutABCDE, Spo1137 and Spo1136 proteins are homologous to ectoine-induced proteins found in *Sinorhizobium meliloti* when this soil bacterium is grown in the presence of ectoine, but their physiological role in ectoine/5-hydroxyectoine degradation by *S. meliloti* has been studied only to some extent.[29]

The UehA protein of *S. pomeroyi* DSS-3 is predicted to encode a periplasmic ESR with 58% amino acid sequence identity to the functionally characterized ectoine/5-hydroxyectoine-binding protein TeaA from *H. elongata*.[15] The small integral membrane component (UehB) of the TRAP system exhibits 56% amino acid sequence identity to TeaB, and the large integral membrane component (UehC) exhibits 74% amino acid sequence identity to TeaC. Prediction of the transmembrane topology[30] revealed 4 and 12 membrane-spanning segments for the UehB and UehC proteins, respectively, a topological arrangement that is typical for the membrane-embedded large and small subunits of TRAP-type transporters.[6–8]

Substrate-induced uptake of [^{14}C]ectoine into *S. pomeroyi* DSS-3

The genes encoding transport systems for nutrients in microorganisms are often induced by their

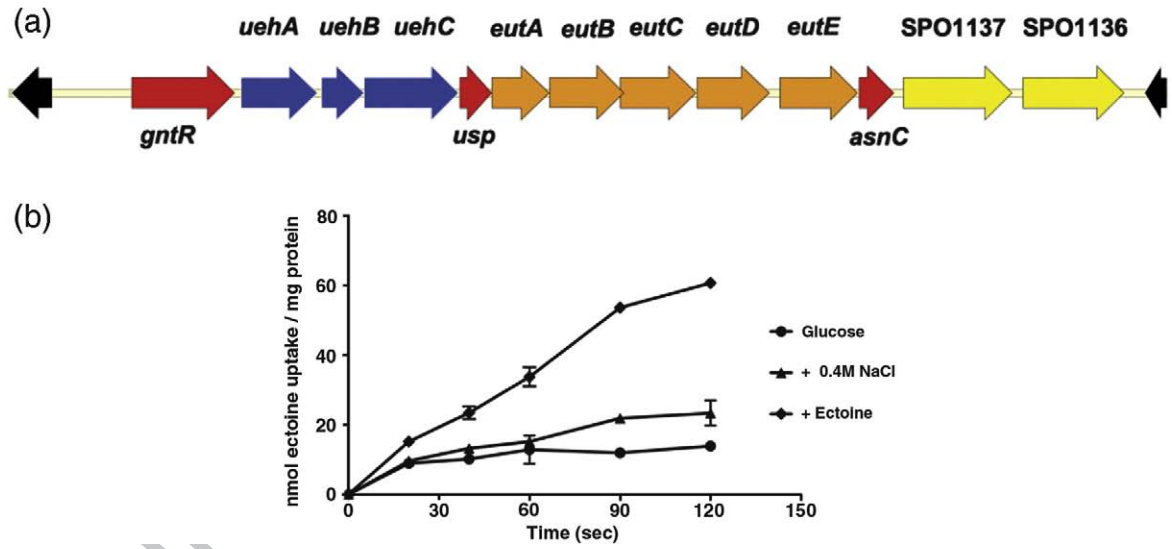

Fig. 1. Genome organization of the *ueh-eut* region and ectoine uptake of *S. pomeroyi* DSS-3. (a) Schematic summary of the *ueh-eut* gene cluster present in *S. pomeroyi* DSS-3. The *uehABC* genes encoding the components for a TRAP-type ectoine/5-hydroxyectoine transport system are flanked by genes encoding a GntR-type regulator and a member of the Usp family. The *usp* gene is followed by five genes (*eutABCDE*) that have been implicated in the utilization of ectoine in *S. meliloti*. The *eut* genes are followed by a gene (*asnC*) encoding a regulator for amino acid metabolism in microorganisms. The two genes (*spo1137* and *spo1136*) following *asnC* possibly encode a succinate-semialdehyde dehydrogenase and an aminotransferase that might also be involved in the degradation of ectoine/5-hydroxyectoine, since such types of proteins are induced when *S. meliloti* is grown in the presence of ectoine. (b) Uptake of [^{14}C]ectoine by cells of *S. pomeroyi* DSS-3. Cultures of *S. pomeroyi* DSS-3 were grown in a shaking water bath in basal minimal medium at 30 °C with either glucose or ectoine as the sole carbon source. A third culture was grown with glucose as the carbon source and an elevated concentration of salt (total concentration of NaCl = 0.4 M). [^{14}C]Ectoine was added to 2-ml aliquots of the cells at a final substrate concentration of 19 μM, and scintillation counting was used to monitor the initial uptake of the radiolabeled ectoine. The data shown are the means of two independently grown cultures in which [^{14}C]ectoine uptake was measured twice per culture.

Please cite this article as: Lecher, J. *et al.*, The Crystal Structure of UehA in Complex with Ectoine—A Comparison with Other TRAP-T Binding Proteins, *J. Mol. Biol.* (2009), doi:10.1016/j.jmb.2009.03.077

cognate substrates (e.g., the maltose ABC transporter of *Escherichia coli*).[1,2] The abovementioned physiological data on the use of ectoine and 5-hydroxyectoine as nutrients, but not as osmoprotectants, suggest that ectoine uptake by *S. pomeroyi* DSS-3 might be induced in cells that are grown in the presence of ectoine. In contrast, ectoine transport should not be enhanced when *S. pomeroyi* DSS-3 is grown in high-salinity media. *S. pomeroyi* DSS-3 was grown (i) in minimal medium with glucose as the sole carbon source, (ii) in minimal medium with a total NaCl content of 0.4 M and (iii) in minimal medium with ectoine as the sole carbon source to test this hypothesis. The various *S. pomeroyi* DSS-3 cultures were grown at 30 °C to mid-exponential phase. The uptake of radiolabeled ectoine was subsequently measured over time by the addition of [^{14}C]ectoine (final concentration = 19 μM). As shown in Fig. 1b, ectoine uptake was very low in either glucose-grown or high salinity-grown cells but was strongly enhanced when the cells were pregrown with ectoine as the sole carbon source. Hence, *S. pomeroyi* DSS-3 possesses a high-affinity ectoine transport activity that is substrate inducible but not osmotically stimulated.

Overproduction and purification of the UehA protein

The sequence relatedness of the UehA ESR from *S. pomeroyi* DSS-3 to the functionally characterized ectoine/5-hydroxyectoine-binding protein TeaA from *H. elongata*[15,23] suggested to us that the UehA protein might recognize both ectoine and 5-hydroxyectoine as its ligands. The UehA protein was overexpressed with an N-terminal *Strep*–tag II affinity peptide in *E. coli* and purified to apparent homogeneity by affinity chromatography on a *Strep*–Tactin column (Fig. 2a) to verify this. The oligomeric composition of the purified UehA protein was analyzed by size-exclusion chromatography. The UehA protein (calculated molecular mass = 34 kDa) eluted from the gel-filtration column as a 36-kDa protein species (Fig. 2b), indicating that UehA is a monomer in solution. UehA shares this property with all other functionally characterized ESR proteins from TRAP-Ts except for the TakP protein from *R. sphaeroides* and the ESR binding protein from *T. maritima*, both being dimeric in solution.[13,16]

Substrate specificity and binding affinities of UehA for ectoine and 5-hydroxyectoine

The binding of ectoine and 5-hydroxyectoine by the purified UehA protein was tested through the use of an intrinsic tryptophan fluorescence-based binding assay.[24,31,32] Addition of increasing concentrations of either ectoine or 5-hydroxyectoine to the UehA protein resulted in a decrease in the intensity of the tryptophan fluorescence, demonstrating that UehA binds both tetrahydropyrimidines. In contrast, the addition of the compatible solutes proline, glycine betaine and trehalose did not elicit any change in the intensity of the tryptophan fluorescence emitted by UehA (data not shown). Consequently, UehA from *S. pomeroyi* DSS-3 is a ligand-binding protein that is specific for ectoine and 5-hydroxyectoine as predicted from the amino acid sequence relatedness to TeaA from *H. elongata*.[23]

Based on the 1:1 Langmuir binding isotherm, K_d values of 1.4 ± 0.1 and 1.1 ± 0.1 μM were calculated for ectoine and 5-hydroxyectoine, respectively (Fig. 3a and b). Hence, the binding affinities of UehA for both ectoine and 5-hydroxyectoine are comparable

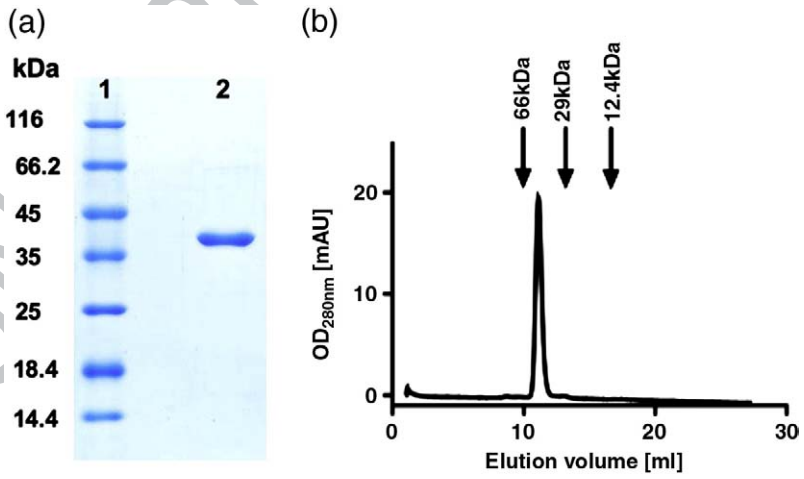

Fig. 2. Analyses of the purified UehA. (a) SDS-PAGE of the purified *S. pomeroyi* DSS-3 UehA protein produced in *E. coli*. Samples of the marker proteins (lane 1) and of UehA (lane 2) were electrophoretically separated on 12.5% SDS-polyacrylamide gel, and the proteins were stained with Coomassie brilliant blue. (b) Determination of the apparent molecular mass of the purified UehA protein by gel-filtration chromatography on a Superdex 75 10/300 column. The protein molecular weight standards used to calibrate the gel-filtration column are indicated by arrows (cytochrome C = 12.4 kDa; carbonic anhydrase = 29 kDa; serum albumin = 66 kDa). The UehA protein eluted from the gel-filtration column with the calculated molecular mass of 36 kDa.

Please cite this article as: Lecher, J. *et al.*, The Crystal Structure of UehA in Complex with Ectoine—A Comparison with Other TRAP-T Binding Proteins, *J. Mol. Biol.* (2009), doi:10.1016/j.jmb.2009.03.077

with those of the homologous *H. elongata* TeaA protein, whose binding properties were analyzed by isothermal titration calorimetry (K_d of 0.19±0.02 μM for ectoine and that of 3.8±0.07 μM for 5-hydroxyectoine).[15] Furthermore, the binding affinities of UehA resemble those of the SBP EhuB of the ABC transporter EhuABC from *S. meliloti* (K_d of 1.6±0.3 μM for ectoine and that of 0.5±0.1 μM for 5-hydroxyectoine).[24] The affinities for both ligands are basically identical in UehA and EhuB, but TeaA apparently binds ectoine with a 20-fold higher affinity than 5-hydroxyectoine.[15]

Overall structure of the UehA–ectoine crystal complex

A native dataset of the UehA–ectoine complex was collected at beamline ID-23 (ESRF, Grenoble, France) and scaled using XDS.[33] Initial phases were obtained by molecular replacement using the program PHASER[34] with the crystal structure of *H. elongata* ectoine-binding protein TeaA as a template [Protein Data Bank (PDB) entry 2vpn].[15] The final structure was refined to a resolution of 2.9 Å. Data and refinement statistics and model content are summarized in Table 1. The overall structure of UehA in complex with ectoine is depicted in Fig. 4a. As expected for a TRAP-T binding protein, UehA is composed of two domains, which are shown in blue (domain I, residues 1–121 and 212–243) and light brown (domain II, residues 122–211 and 244–310), respectively, in the figure. Each of these domains is composed of a central antiparallel five-stranded β-sheet. Furthermore, domain I contains six α-helices, while domain II harbors eight α-helices and one additional β-strand (Fig. 4a and b), which flank the central sheet on both sites. Interestingly, one strand forms the central β-sheets of the two domains, thereby crossing the whole protein.

The remarkable features of the UehA structure are reflected in the topology diagram of UehA (Fig. 4b). Both domains contain the mentioned five-stranded antiparallel β-sheets, which have the orders BACJD and GFHEI, respectively. This strand order is found in all other ESR proteins of TRAP-Ts and in class II ABC-dependent SBPs.[35] However, not only the strand order but also the additional β-strand and

Table 1. Crystallographic parameters

Crystal parameters at 100 K	
Space group	$P2_1$
Unit cell parameters	
a, *b*, *c* (Å)	63.0, 61.3, 86.3
β (°)	102.6
Data collection and processing	
Wavelength (Å)	0.87260
Resolution (Å)	30–2.9 (2.97–2.9)
Mean redundancy	4.0 (3.7)
Unique reflections	14,412
Completeness (%)	99.6 (99.7)
I/σ	11.3 (3.6)
R_{sym}	11.0 (42.9)
Refinement statistics	
R_F (%)	21.8
R_{free} (%)	26.2
rmsd from ideal	
Bond lengths (Å)	0.007
Bond angles (deg.)	0.97
Average *B*-factors (Å^2)	43.1
Ramachandran plot	
Most favored (%)	91.0
Allowed (%)	8.3
Generously allowed (%)	0.7
Disallowed (%)	—
Model content	
Monomers/ASU	2
Protein residues	1–310
Ligand	2 ectoines
Other	—

Crystal parameters and data collection statistics were derived from XDS. Refinement statistics were obtained from REFMAC5, and Ramachandran analysis was performed using PROCHECK.

[a] $R_{sym} = \frac{\sum_{hkl}\sum_i |I_i(hkl) - \langle I(hkl)\rangle|}{\sum_{hkl}\sum_i I_i(hkl)}$.

[b] $R_F = \sum_{hkl} ||F_o| - |F_c|| / \sum_{hkl} |F_o|$. R_{free} is calculated as R_F but for 5% randomly chosen reflections that were omitted from all refinement steps.

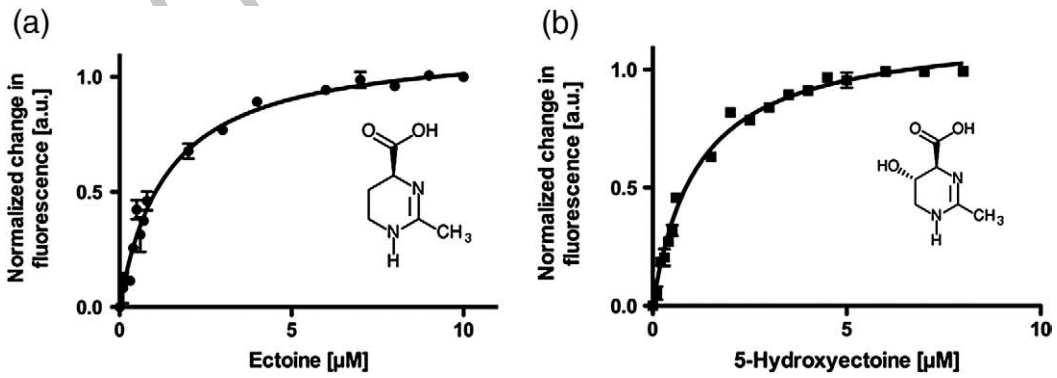

Fig. 3. Dissociation constant of the UehA–ectoine complex. Equilibrium binding titration experiments with ectoine (a) or 5-hydroxyectoine (b) to purified UehA were performed using an intrinsic tryptophan fluorescence-based binding assay. The chemical structures of ectoine and 5-hydroxyectoine are shown in the inset. Equilibrium binding assays were performed in triplicate, and data were analyzed as outlined in Materials and Methods.

Please cite this article as: Lecher, J. *et al.*, The Crystal Structure of UehA in Complex with Ectoine—A Comparison with Other TRAP-T Binding Proteins, *J. Mol. Biol.* (2009), doi:10.1016/j.jmb.2009.03.077

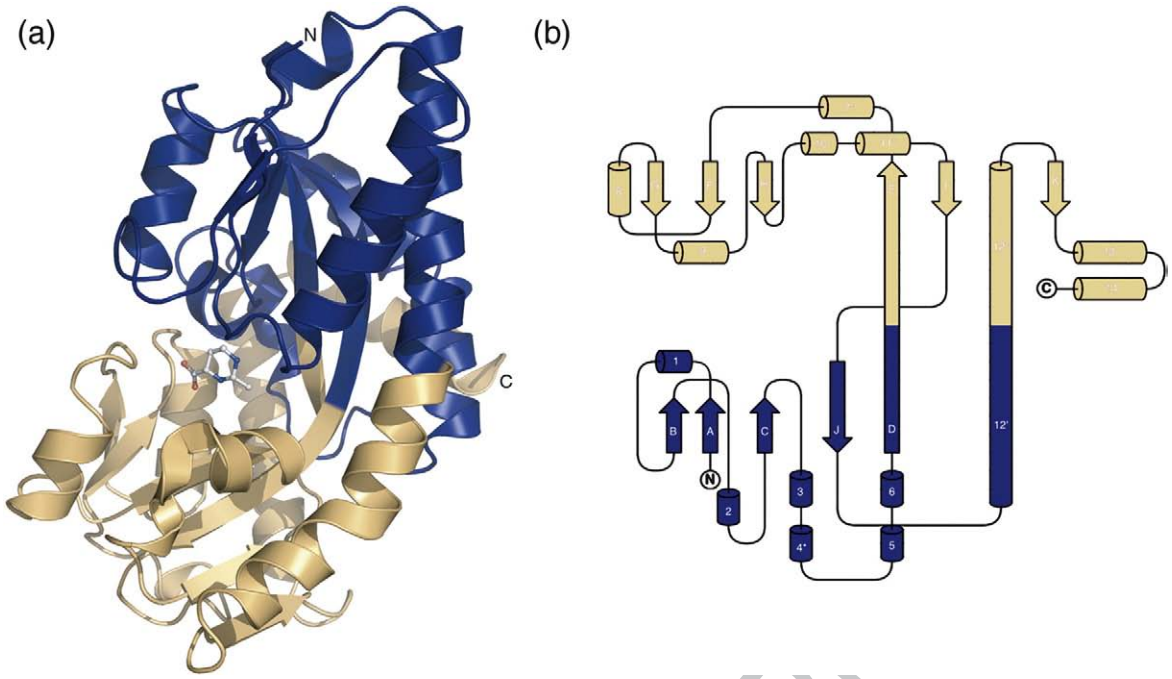

Fig. 4. Overall structure of UehA in complex with ectoine. (a) Domain I of UehA is shown in blue, and domain II of UehA is shown in light orange. The ectoine ligand is shown in ball-and-stick representation. The N- and C-termini are labeled. (b) A topology diagram of UehA where domain I is in blue and domain II is in dark orange. Helices are labeled by numbers; β-strands, by letters. 3_{10}-Helices are indicated by an asterisk.

the number and positioning of the flanking α-helices are conserved in all TRAP-dependent ESRs structurally characterized so far. Quite striking is the long helix (residues 225–260) of UehA lying on top of the protein spanning both domains of UehA. Such a long helix is found in all crystal structures of ESR proteins reported so far from TRAP-Ts, although in some structures this helix is interrupted by a kink.[16]

The ectoine ligand-binding site in UehA

The ligand ectoine resides in a deep cleft located between both domains of UehA (Fig. 4a). Despite the modest resolution of the UehA structure (2.9 Å), the orientation of ectoine within the ligand-binding site could be determined unambiguously as demonstrated by a $1F_o - F_c$ omit map contoured at 3σ (Fig. 5). Residues from both domains (shown in blue and yellow in Fig. 5) of UehA form the ectoine-binding site: one ligand-interacting residue is provided by domain I, and five ligand-interacting residues originate from domain II. Hence, residues from both domains of UehA stabilize and orient the ligand within the binding pocket, a general feature found in ESRs and SBPs. Three salt bridges contribute to the stabilization and positioning of ectoine within the UehA ligand-binding pocket: the carboxyl moiety of ectoine interacts with Arg144, the imido moiety of ectoine interacts with Glu9 and, furthermore, the imido and carboxylate moieties of ectoine both interact with Asn184. In addition, cation–pi interactions of the delocalized positive charge of ectoine are formed by Trp167, Phe188 and Phe209 of UehA and make important contributions to ligand binding. Hydrophobic interactions of ectoine with Glu8, Phe66, Met146 and Phe187 provide further stabilization of the ligand (Fig. 5).

Compatible solutes are usually excluded from the immediate hydration shell of proteins due to unfavorable interactions with the protein backbone.[36] However, in ESRs and SBPs, high-affinity interactions with the ligand (K_d values in the low micromolar or even nanomolar range) are required to permit the efficient scavenging of compatible solutes from scarce environmental sources. The crystal structures of several compatible solute binding proteins have recently been determined in complex with their specific ligands.[24,31,32,37–39] A combination of direct (salt bridges and hydrogen bonds) and non-direct (cation–pi) interactions has been observed at a structural level not only in the ectoine-specific ESRs UehA and TeaA but also in ABC-dependent SBPs with specificity for compatible solutes, such as glycine betaine, proline betaine and dimethylsulfonioacetate. Examples include the ectoine/5-hydroxyectoine-binding protein EhuB from *S. meliloti*,[24] the glycine betaine–proline betaine–dimethylsulfonioacetate binding protein OpuAC from *Bacillus subtilis*,[31,37] the choline–acetylcholine binding protein ChoX from *S. meliloti*[32] and the glycine betaine–proline betaine binding protein ProX from *E. coli* and that from *Archaeoglobus fulgidus*.[38,39] Hence, in SBP and ESR originating

Please cite this article as: Lecher, J. *et al.*, The Crystal Structure of UehA in Complex with Ectoine—A Comparison with Other TRAP-T Binding Proteins, *J. Mol. Biol.* (2009), doi:10.1016/j.jmb.2009.03.077

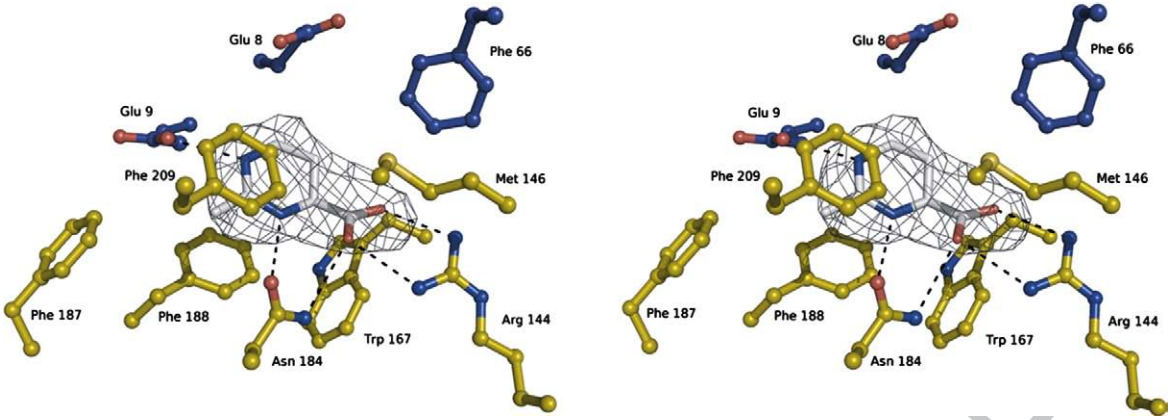

Fig. 5. The ectoine ligand-binding site in UehA. Residues of domain I of UehA participating in ligand binding are shown in blue and residues originating from domain II of UehA are shown in orange, and the numbers of the amino acids forming the ligand-binding pocket are labeled. The ectoine ligand is shown in ball-and-stick representation. Hydrogen bonds and salt bridges are highlighted by black dashed lines. The gray mesh indicates a $1F_o - F_c$ omit electron density map of the ectoine ligand-binding site contoured at 3σ. For electron density map calculations, the ligand was omitted from the refinement.

from a diverse range of microbial species, common types of molecular interactions are employed to efficiently and specifically bind compatible solutes within binding pockets.

Comparison of the UehA structure with the ectoine-binding ESR TeaA

The ESR UehA from *S. pomeroyi* DSS-3 and TeaA from *H. elongata* are each part of an ectoine/5-hydroxyectoine-specific TRAP-T system. However, their physiological functions differ: TeaABC is involved in the acquisition of ectoine/5-hydroxyectoine as osmoprotectants from environmental sources,[23] whereas the UehABC system serves as an ectoine/5-hydroxyectoine transporter for nutritional purposes (Fig 1b). Several uptake systems for compatible solutes, such as the ABC transporter OpuA from *Lactococcus lactis*,[40] the BCCT-type transporter BetP from *Corynebacterium glutamicum*[41] and the MFS-type transporter ProP from *E. coli*,[42] are regulated at the level of transport activity by high osmolarity. These transport systems respond to a sudden osmotic up-shock with increased import of compatible solutes to protect the microbial cells from the detrimental effects of high osmolarity. Such a response via the UehABC system is quite unlikely because both ectoine and 5-hydroxyectoine simply do not serve as osmoprotectants for *S. pomeroyi* DSS-3. These tetrahydropyrimidines, in contrast to the metabolically inert osmoprotectant glycine betaine, only serve as nutrients in *S. pomeroyi* DSS-3 (J.B. and E.B., unpublished results); consequently, there is no physiological need for the cell to regulate ectoine and 5-hydroxyectoine uptake in response to increased osmolarity of the environment.

Despite these physiologically different functions, the TeaA and UehA proteins are closely related in amino acid sequence (62% amino acid sequence identity and 82% homology), and this close relatedness is reflected in the crystal structures of both proteins. A structural superposition of UehA and TeaA reveals an rmsd of 0.8 Å over 309 C^{α} atoms (data not shown). Besides the overall fold, the architectural arrangements of the residues interacting with the ectoine ligand are also identical in UehA (Fig. 5) and TeaA (data not shown). The crystal structure of the TeaA–ectoine complex was refined by Kuhlmann *et al*. to a resolution of 1.55 Å.[15] This high resolution allowed the conclusion that residues Glu44 and Ser45 of TeaA interact indirectly with the ectoine ligand via a bridging water molecule. Since the UehA structure reported here was determined only at modest resolution (2.9 Å), we refrained from including water models in our final model. However, given the close amino acid sequence and structural relatedness of UehA and TeaA, it seems reasonable to assume that a bridging water molecule might also mediate similar interactions of Glu44 and Ser45 in UehA with the ectoine ligand. Remarkably, despite the different physiological tasks performed by the TeaABC and UehABC transporters, nature has chosen the same architecture of the substrate-binding site in TeaA and UehA to effectively capture the ligand ectoine.

The structure of TeaA revealed a pronounced negatively charged surface. However, the moderate halophile *H. elongata* can grow over a wide range of salinities (up to 10% NaCl). Such an exposure of negative charges to the surface is common among proteins of extremely halophilic archaea.[15] Interestingly, the surface of UehA also contains mainly negatively charged amino acids, although *S. pomeroyi* DSS-3 lives in a marine habitat, an environment of moderately elevated salinity (approximately 3.5% NaCl) (data not shown).

Comparison of the ESR UehA with the ectoine-binding SBP EhuB

The EhuB protein is part of an ABC transport system that serves for the uptake of ectoine and 5-

Please cite this article as: Lecher, J. *et al.*, The Crystal Structure of UehA in Complex with Ectoine—A Comparison with Other TRAP-T Binding Proteins, *J. Mol. Biol.* (2009), doi:10.1016/j.jmb.2009.03.077

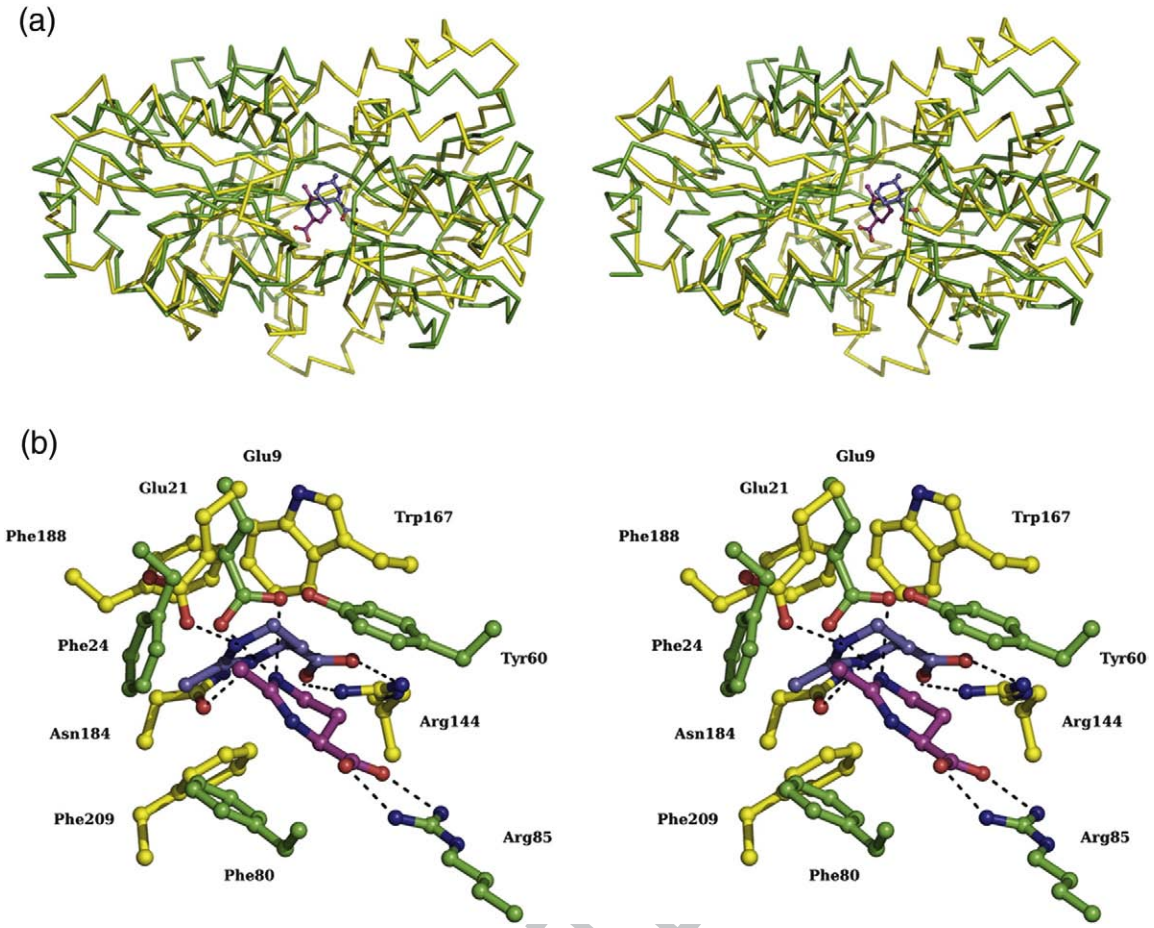

Fig. 6. Structural superposition of the EhuB and UehA ectoine-binding proteins. (a) Stereo view of a structural superposition of the SBP EhuB (green) from *S. meliloti* and the ESR UehA from *S. pomeroyi* (yellow). The ectoine ligand is shown in ball-and-stick representation in either magenta for EhuB or dark cyan for UehA. (b) Detailed view of the ectoine ligand-binding site in EhuB and UehA. The overall structures of EhuB and UehA were used as a reference point for the comparison of the ectoine ligand-binding sites. Residues that directly interact with ectoine and the ligands are shown in ball-and-stick representation. Hydrogen bonds and salt bridges between the ligand and the protein are highlighted by black dashed lines. The color coding for residues originating from either EhuB or UehA is identical with that shown in (a).

hydroxyectoine for nutritional purposes in the soil bacterium *S. meliloti*.[29] The crystal structure of EhuB was solved in complex with either ectoine or 5-hydroxyectoine.[24] In their recent structural analysis of TeaA, Kuhlmann *et al.*[15] compared TeaA and EhuB by superimposing the common ligand ectoine. Applying this strategy, they detected significant differences in the architecture of the ligand-binding site and mode of ligand binding between the EhuB and TeaA proteins. However, when we followed this approach by using the ectoine ligand bound by UehA as the anchor point for the EhuB–UehA comparison, we found a clear misalignment of the protein backbone of both proteins (data not shown). Therefore, we used the protein structure of UehA and EhuB for an overall superposition (Fig. 6a). This resulted in an rmsd of 3.0 Å for 162 C^{α} atoms (Fig. 6a). In this superposition, it is evident that the central antiparallel β-sheets of both domains align well, while the long helix 12 (Fig. 4b) and the helices

Fig. 7. Structural superposition of TRAP-derived SBPs. (a) Ribbon representations of a structural superimposition of UehA (orange) and SiaP (yellow). The ligands ectoine in UehA and sialic acid in SiaP are shown in ball-and-stick representation. (b) Detailed views of the structure of the ligand-binding sites present in UehA (orange) and SiaP (yellow). Residues forming the ligand-binding site and the ligands are shown in ball-and-stick representation. Helix 3 is displayed in cartoon representation. Residues lining the binding side are labeled. Here, the first residue always refers to UehA; the second, to the structurally corresponding residue of SiaP. If no corresponding residue was present, only a single residue is indicated. (c) The structures of UehA (orange) and TakP (cyan) are superimposed and represented as ribbons. The ligands ectoine (UehA) and pyruvate (TakP) are shown in ball-and-stick representation. (d) Detailed views of the ligand-binding site of UehA (orange) and TakP (cyan) are presented. Residues forming the ligand-binding site and the ligands are shown in ball-and-stick representation. Helix 3 is displayed in cartoon representation. Residues lining the binding side are labeled. Here, the first residue always refers to UehA; the second, to the structurally corresponding residue of TakP. If no corresponding residue was present, only a single residue is indicated.

Please cite this article as: Lecher, J. *et al.*, The Crystal Structure of UehA in Complex with Ectoine—A Comparison with Other TRAP-T Binding Proteins, *J. Mol. Biol.* (2009), doi:10.1016/j.jmb.2009.03.077

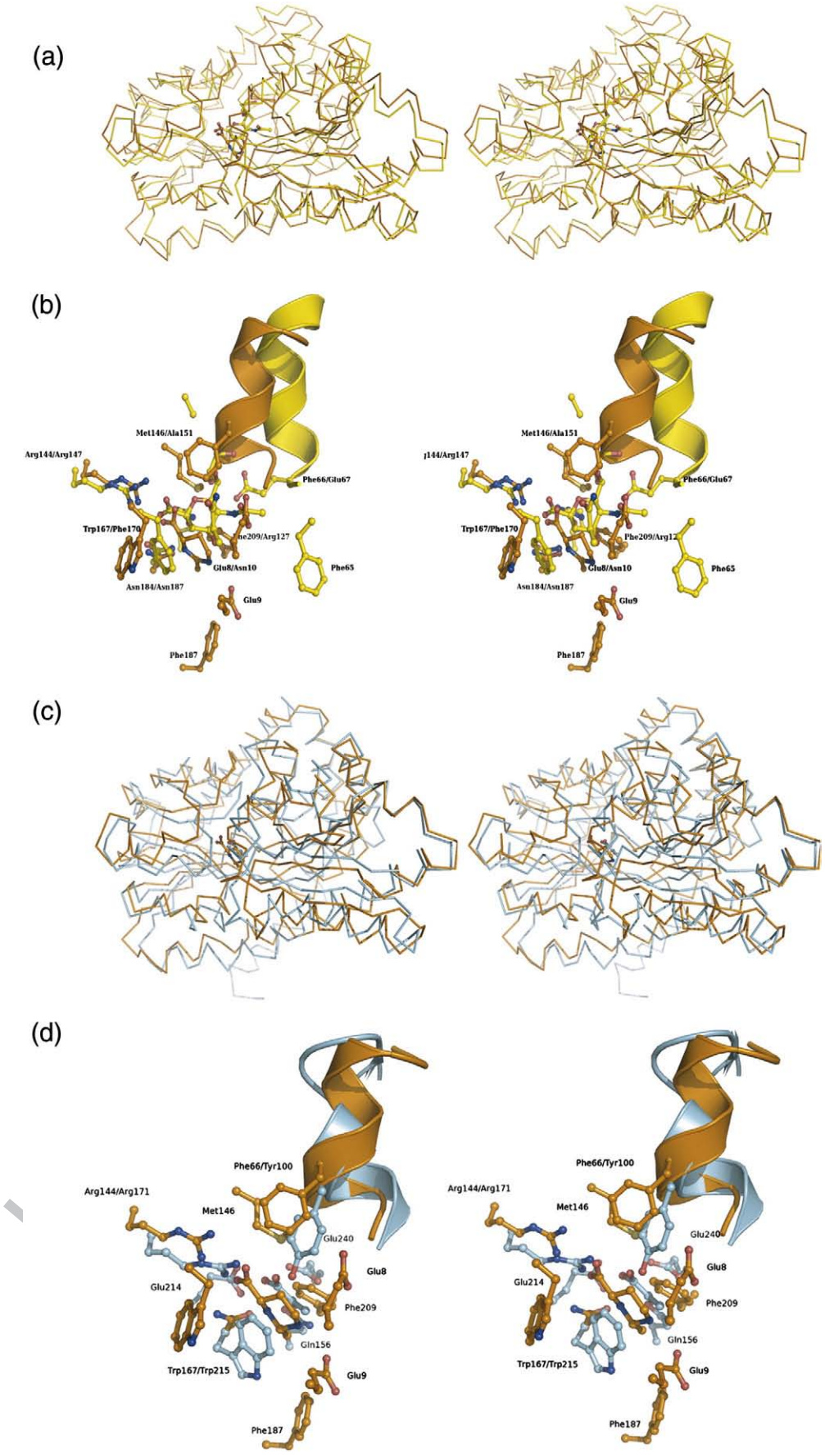

Fig. 7 *(legend on previous page)*

Please cite this article as: Lecher, J. *et al.*, The Crystal Structure of UehA in Complex with Ectoine—A Comparison with Other TRAP-T Binding Proteins, *J. Mol. Biol.* (2009), doi:10.1016/j.jmb.2009.03.077

of the C-terminal part of UehA (Fig. 6a) have no counterpart in EhuB. The alignment of the core part of both proteins underlines the structural similarities of SBPs from ABC transporters and ESRs from TRAP-Ts. It has already been suggested that both types of ligand-binding proteins evolved from a common ancestor and perform similar functions in ABC- and TRAP-type transporters.[8,17]

Figure 6b represents a detailed view of the aligned ectoine-binding site present in UehA (yellow) and in EhuB (green). The ligands are displayed in ball-and-stick representation in cyan for UehA and in magenta for EhuB. In our alignment approach, which used the protein backbones as anchor points, a detailed view of the binding site clearly demonstrates that the positions of the ectoines are different in UehA and EhuB. Both a rotational shift and a translational shift would be required to adequately superimpose the ligands. Despite these shifts, the ligand–protein interactions in UehA and EhuB are identical. The carboxylate of ectoine interacts with an arginine residue (Arg144 in UehA and Arg85 in EhuB), and the imido moiety interacts with a glutamate (Glu9 in UehA and Glu21 in EhuB). Additionally, a hydrogen bond is present between Asn184 and the imido moiety of ectoine in UehA, but there is no counterpart for this type of interaction in EhuB. These protein–ligand contacts are completed by cation–pi interaction between the delocalized positive charges of the ectoine ligands and aromatic residues present in the two binding proteins. However, these aromatic residues in UehA and EhuB are swapped between the domains: they originate from domain I in EhuB and from domain II in UehA. Another interesting swap occurred for the arginine residue that interacts with the carboxylate moiety of ectoine. Arg144 of UehA is structurally conserved in all ESRs of TRAP-Ts that were structurally characterized so far.[12–16] The same holds true for Arg85 of EhuB, which is equally conserved in binding proteins from ABC transporters likely being involved in ectoine uptake.[24] However, as in the case of the aromatic residues participating in cation–pi interactions, the two arginines stem from different domains: domain I in EhuB and domain II in UehA. In both the UehA and EhuB structures, the ligand is completely shielded from the solvent and buried deep within the protein. Thus, both proteins employ the same principles of ligand binding and generate an overall architecture to perfectly accommodate ectoine, but the detailed arrangements of the amino acid residues forming the ligand-binding site are different in UehA and EhuB.

Structural comparison of UehA with ESRs of other TRAP-Ts

Recently, the crystal structures of seven TRAP-associated ESRs have been characterized by X-ray crystallography. A comparison of each of these structures with UehA (Fig. 7) revealed that all TRAP-dependent ESRs analyzed by X-ray crystallography adopt the same overall tertiary structure. Not only are the topological arrangements of the central β-sheets identical but also the number of the flanking helices and their structural arrangement are virtually superimposable. This also includes the extended helix (helix 12 in UehA; see Fig. 4a) spanning in each case the whole ESR structure.

As an example of this remarkable structural similarity between the ESRs of TRAP systems with different substrate specificities, structural alignments of UehA with the *N*-acetyl-5-neuramic acid-specific binding protein SiaP[12,17] and the α-keto acid-specific binding protein TakP[13] are shown in Fig. 7. The overlay of UehA (orange) and SiaP (yellow) is provided in Fig. 7a. Both proteins align with an rmsd of 2.1 Å over 310 C^{α} atoms, despite the fact that the amino acid sequence homology between UehA and SiaP is only 26%. Another example is provided in Fig. 7c. Here, UehA and TakP were superimposed, resulting in an rmsd of 2.4 Å over 310 C^{α} atoms (the amino acid sequence identity between these two proteins is only 18%). Structural alignments of UehA with other ESRs revealed similar values, indicating that the overall structure of all TRAP-dependent ESRs is, within experimental error, identical, and this includes the number and orientation of the flanking helices in these binding proteins as well.

The common structural architecture of TRAP-associated ESRs implies that these SBPs might all interact in the same way with the membrane components of TRAP-type transport systems. However, significant functional differences seem to exist with respect to the oligomeric composition of the various ESRs in solution and in crystals. Both the TakP protein from *R. sphaeroides*[13] and the ESR from *T. maritima*[16] form dimers in solution. Elaborate models have been proposed to explain how such a dimeric complex of the ESR might channel the ligand to the membrane components of the TRAP system for solute import. The other ESRs, for which structural information is available, are all monomers in solution, and it is thus likely that these ligand-binding proteins also interact as monomers with the cognate membrane components of the various TRAP-Ts. UehA belongs to this latter group since it elutes as a monomer from a size-exclusion column (Fig. 2b). A monomeric SBP is also observed in the crystal structures of three microbial ABC importers in complex with their cognate ligand-binding proteins. In these structures, a monomeric binding protein interacts simultaneously with both transmembrane components of the ABC transporter.[43–45]

The structural relatedness of the various ESRs from TRAP-Ts raises the question of how substrate specificity for the ligand is generated within this protein family. Detailed structural comparisons of the ligand-binding sites of UehA–SiaP and UehA–TakP are provided in Fig. 7b and Fig. 7d, respectively. Residues of both proteins that interact with the respective ligand are shown in ball-and-stick representation (orange color coding for UehA and yellow color coding for SiaP in Fig. 7b), and the

Please cite this article as: Lecher, J. *et al.*, The Crystal Structure of UehA in Complex with Ectoine—A Comparison with Other TRAP-T Binding Proteins, *J. Mol. Biol.* (2009), doi:10.1016/j.jmb.2009.03.077

corresponding ligands (ectoine in UehA and *N*-acetyl-5-neuramic acid in SiaP) are shown in ball-and-stick representation in orange and yellow, respectively.

The well-conserved arginine residues (Arg144 in UehA and Arg147 in SiaP) perfectly align in this structural comparison. Other residues such as Asn184 (UehA) and Asn187 (SiaP) or Trp167 (UehA) and Phe170 (SiaP) also correspond, whereas certain residues such as Glu9 (UehA) are specific for the particular ESR. These specific interactions are likely a consequence of the chemical structure of the ligand that has to be complexed by a given ESR. However, most striking in this comparison is the positioning of helix 3 in the various ESRs. The exact positioning of this helix in UehA prohibits binding of sialic acid (a substrate for SiaP) because of a steric clash between the side chain of the ligand and the backbone of the helix. Furthermore, in both the UehA and SiaP proteins, one residue of helix 3 participates in ligand binding: these are Phe66 in UehA and Glu67 in SiaP. Thus, the exact position of helix 3 is a critical determinant for the size of the ligand-binding pocket, thereby significantly contributing to the precise positioning of the individual ligands within the binding site.

A similar situation is observed when one compares the ligand-binding sites of UehA (orange) with those of TakP (cyan; Fig. 7d), an ESR that is specific for α-keto acids. Again, the two conserved arginine residues align fairly well (Arg144 in UehA and Arg171 in TakP) and in both proteins two residues originating from helix 3 (Phe66 in UehA and Tyr100 in TakP) interact with the ligand. Since ectoine and pyruvate are of similar size, the position of helix 3 is comparable in both proteins and the displacement of this helix observed by comparing the UehA and SiaP structures is less pronounced. Nevertheless, in all structures analyzed, helix 3 adopts a specific and unique position within the family of TRAP-associated ESRs. Our analysis of the available structures of these types of proteins strongly suggests that helix 3 acts as a "selectivity helix" by modulating the volume available for a given ligand within the binding pocket and that helix 3 provides at least one residue that directly interacts with the given ligand.

UehA as a structural and functional template for other putative ectoine-binding proteins from TRAP transport systems

A BLAST search[46] for proteins from both bacteria and archaea that are related to the amino acid sequence of the *S. pomeroyi* DSS-3 UehA protein was conducted using the DOE Joint Genome Institute Web server‡. Proteins that are similar to UehA were readily detected, and the top 10 UehA-related proteins were retained for further analysis and their amino acid sequences were aligned using the ClustalW algorithm[47] (see Supplementary Fig. 1). Each of these proteins originates from Gram-negative bacteria and contains an N-terminal signal sequence that directs it via the Sec pathway into the periplasmic space. The 10 UehA-related proteins are each encoded as part of a gene cluster (*dctPQM*) whose products are annotated as DctPQM-type TRAP transport systems. They all stem from microorganisms belonging to the proteobacteria, and all live in either marine or saline habitats. These microorganisms comprise *Roseobacter* spp. (two species), *Marinobacter* spp. (three species) and species from the *Oceanibulbus*, *Oceanicola*, *Aurantimonas*, *Fulvimarina*, *Halomonas* and *Reinekea* genera.

These ESR proteins all align with the UehA protein from *S. pomeroyi* DSS-3 without any gaps, comprise a similar number of amino acids and exhibit a degree of amino acid sequence identity with UehA that ranges from 74% to 96% (see Supplementary Fig. 1). We then inspected the aligned UehA-related proteins for the conservation of those nine amino acid residues that form the ectoine-binding pocket in the UehA structure (Fig. 5). Eight of the ligand-interacting residues present in UehA are fully conserved. A minor variation occurs at a position that corresponds to Phe188 in UehA; at this site, the Phe residue is conservatively replaced by either Tyr or Trp residues in some proteins. The strict conservation of the ligand-interacting residues from UehA in the compiled and aligned proteins strongly suggests that each of these ESRs is actually an ectoine-binding protein with an overall structure resembling that of the *S. pomeroyi* DSS-3 UehA protein (Fig. 3a).

This suggestion is strengthened by the finding that not only is the ligand-binding protein conserved but also the small and large integral membrane components of the different TRAP transport systems are related to the corresponding proteins (TeaB–UehB and TeaC–UehC) from the *H. elongata* and *S. pomeroyi* DSS-3 ectoine/5-hydroxyectoine TRAP uptake systems. The amino acid sequence identity of the UehB-related proteins ranges from 48% to 98%, whereas the amino acid sequence identity of those related to UehC ranges from 71% to 96%. The *S. pomeroyi* DSS-3 *uehABC* gene cluster is also followed by a universal stress protein (Usp) *usp* gene (Fig. 1a). Genes encoding homologs of these Usps[48] have been observed to be adjacent to the genes encoding the components of many TRAP-Ts, but their role in connection with TRAP-type transporters has not yet been explored.[8]

Conclusions

Uptake of ectoine and 5-hydroxyectoine in *S. pomeroyi DSS* is mediated by the substrate-inducible TRAP-T UehABC. In contrast to TeaABC from *H. elongata*, the only other functionally characterized TRAP-T for ectoine and 5-hydroxyectoine, the UehABC system is not involved in osmoprotection and instead imports both ectoine and 5-hydroxyectoine for nutritional purposes. The ESR of the

‡ http://www.jgi.doe.gov/

Please cite this article as: Lecher, J. *et al.*, The Crystal Structure of UehA in Complex with Ectoine—A Comparison with Other TRAP-T Binding Proteins, *J. Mol. Biol.* (2009), doi:10.1016/j.jmb.2009.03.077

UehABC system, UehA, binds both ectoine and 5-hydroxyectoine with high specificity and affinity. The structure of UehA in complex with ectoine revealed the molecular determinants for ligand binding. Databank searches identified a group of UehA-related putative ectoine-binding proteins from marine microorganisms in which the residues forming the ligand-binding pocket are strictly conserved, implying that the structure of UehA can serve as template for functional studies of other ectoine-specific ESRs. The ligand-binding pocket of UehA is superimposable to that of the ectoine-binding protein TeaA, and the types of interactions between residues present in UehA–TeaA and its ligand ectoine can also be found in the ectoine-specific SBP EhuB from *S. meliloti*.

We compared the crystal structure of UehA with the structures of seven ESRs originating from TRAP systems with different substrate specificities. The overall fold of all ESRs is virtually identical, and we found that the size of the substrate-binding pocket in these proteins is dictated by only one helix (helix 3). The positioning of this helix modulates the volume of the binding pocket with the ESR and apparently aids in determining the selectivity of ligand binding.

Materials and Methods

Chemicals

Ectoine and 5-hydroxyectoine were obtained from bitop AG (Witten, Germany) and were generous gifts of Dr. T. Schwarz. [^{14}C]Ectoine (4.22 MBq mmol^{-1}) was prepared and purified as detailed previously[49] and was a kind gift of Dr. M. Jebbar (University of Rennes, Rennes, France). Glycine betaine, proline and trehalose were purchased from Sigma-Aldrich (München, Germany). Anhydrotetracycline and desthiobiotin were obtained from IBA (Göttingen, Germany).

Bacterial strains, plasmids and culture conditions

S. pomeroyi DSS-3 (DSM 15171)[20] was obtained from the German Collection of Microorganisms and Cell Cultures (DSMZ; Braunschweig, Germany). *S. pomeroyi* DSS-3 was propagated and maintained on half-strength YTTS complex medium as described previously.[50] For the growth of *S. pomeroyi* DSS-3 in a chemically defined medium, we used the basal minimal medium described previously[51] at 30 °C. This medium had the following composition: 200 mM NaCl, 50 mM $MgSO_4 \times 7H_2O$, 10 mM KCl, 10 mM $CaCl_2 \times 2H_2O$, 190 mM NH_4Cl, 0.33 mM K_2HPO_4, 0.1 mM $FeSO_4 \times 7H_2O$, 50 mM Mops, pH 7.5, 28 mM glucose and 5 ml l^{-1} each of two vitamin solutions. For cells that were grown at elevated salinity, the total concentration of NaCl in the medium was raised to 0.4 M. In cultures of *S. pomeroyi* DSS-3 that used ectoine as the sole carbon source, the glucose content of the basal minimal medium was replaced by 28 mM ectoine. *E. coli* strain BL21(DE3) (Stratagene, La Jolla, CA) was used for the overexpression of the *S. pomeroyi* DSS-3 *uehA* gene carried by the expression plasmid pBJ20, a derivative of the vector pASK-IBA6 (IBA). BL21(pBJ20) strains were propagated on LB–agar plates containing ampicillin (100 μg ml^{-1}). For UehA overproduction, the pBJ20-carrying BL21 strain was propagated in a defined minimal medium (MMA)[52] supplemented with 100 μg ampicillin ml^{-1}, 0.4% (w/v) casamino acids and 0.4% (w/v) glucose as the carbon source with additional 0.2 g l^{-1} of $MgSo_4 \times 7H_2O$ and 1 mg l^{-1} of thiamine.

Uptake assays for [^{14}C]ectoine by *S. pomeroyi* DSS-3 cells

Uptake assays for [^{14}C]ectoine (4.22 MBq mmol^{-1}) by *S. pomeroyi* DSS-3 cells were conducted as described previously by Bursy *et al.*[28] Cells were grown in the basal minimal medium to an OD_{578} of approximately 1.0. Samples of 2 ml were taken, and [^{14}C]ectoine was added to the cells at a final concentration of 19 μM. At the indicated time intervals, 0.3-ml samples were withdrawn and the radiolabeled ectoine taken up by the cells was determined by liquid scintillation counting. Cells grown under the following conditions were used for the [^{14}C] ectoine uptake experiments: (i) basal minimal medium with glucose as the carbon source, (ii) basal minimal medium with glucose as the carbon source and a total NaCl content of 0.4 M and (iii) basal minimal medium with ectoine (28 mM) as the carbon source. Prior to the [^{14}C]ectoine uptake assays, cells were washed two times in basal minimal medium with glucose (28 mM), except for the cells that were pre-grown in the presence of 0.4 M NaCl. For these cells, 0.4 M NaCl was added to the washing solution to prevent an osmotic down-shock of the cells.

Construction of a *uehA* expression plasmid and overproduction and purification of the recombinant UehA protein

Chromosomal DNA of *S. pomeroyi* DSS-3 was prepared using tip-20 QIAGEN columns (QIAGEN, Hilden, Germany). Synthetic oligonucleotides were used to amplify by PCR the *uehA* coding region from the *S. pomeroyi* DSS-3 genomic DNA without the DNA segment specifying the predicted UehA N-terminal signal sequence. The amplified *uehA* DNA segment was ligated into the pASK-IBA6 expression vector yielding plasmid pBJ20. The *uehA* coding region was inserted into pASK-IBA6 in-frame with an upstream *ompA* signal sequence and the codons specifying the *Strep*–tag II affinity peptide. This allowed the secretion of the *Strep*–tag II–UehA fusion protein into the periplasmic space of *E. coli*, from which it could be released by cold osmotic shock and recovered by affinity chromatography on *Strep*–Tactin Sepharose (IBA). The nucleotide sequence of the *uehA* coding region present in plasmid pJB20 was verified by DNA sequence analysis, and this was carried out by Eurofins MWG Operon (München, Germany).

Six 1-l minimal media were inoculated with an overnight culture of strain BL21(pBJ20) and were then incubated in an aerial shaker set at 170 rpm at 32 °C. UehA production was initiated by the addition of the inducer of the *tet* promoter present in pBJ20, anhydrotetracycline (final concentration = 0.2 μg ml^{-1}), at an OD_{578} of 0.7, and growth of the cultures was then continued for two additional hours. Subsequently, the *E. coli* cells were harvested by centrifugation (10 min, 6000*g*). The cell pellet was resuspended in 50 ml ice-cold (4 °C) buffer P (100 mM Tris–HCl, pH 7.5, 1 mM ethylenediaminetetraacetic acid and 500 mM sucrose) and incubated for 30 min on ice to release the periplasmic proteins. Soluble periplasmic

Please cite this article as: Lecher, J. *et al.*, The Crystal Structure of UehA in Complex with Ectoine—A Comparison with Other TRAP-T Binding Proteins, *J. Mol. Biol.* (2009), doi:10.1016/j.jmb.2009.03.077

proteins were isolated by two subsequent centrifugation steps. First, the supernatant was centrifuged for 15 min at 21,000*g* to remove cellular debris. Subsequently, the supernatant was recentrifuged for 60 min at 120,000*g* to remove denatured proteins and fragments of the cell membrane. The soluble periplasmic protein fraction was then loaded onto a 10-ml *Strep*–Tactin Sepharose column (IBA) pre-equilibrated with 5 bed volumes of buffer W (100 mM Tris–HCl and 100 mM NaCl, pH 7.5). After the column was washed with 5 bed volumes of buffer W, proteins bound to the affinity matrix were eluted with 3 bed volumes of buffer E (100 mM Tris–HCl, pH 7.5, 100 mM NaCl and 2.5 mM desthiobiotin) from the column. UehA-containing fractions were collected in 3-ml aliquots, and their protein content was analyzed by SDS-PAGE. UehA protein used for crystallization experiments was concentrated to approximately 12 mg ml^{-1} by using Vivaspin 4 (Vivascience, Hannover, Germany) concentrator columns (exclusion size = 10 kDa) in a buffer containing 10 mM Tris–HCl, pH 7.5, and 10 mM NaCl.

Size-exclusion chromatography of UehA

The oligomeric composition of the purified UehA protein was determined by size-exclusion chromatography on a Superdex 75 10/300 column (GE Healthcare, München, Germany). The column was equilibrated and run with 10 mM Tris–HCl, pH 7.5, and 100 mM NaCl, and the elution profile of proteins was monitored at a wavelength of 280 nm using an ÄKTA Purifier System (GE Healthcare). The following marker proteins were used: cytochrome *C* (12.4 kDa), carbonic anhydrase (29 kDa) and serum albumin (66 kDa) (Sigma-Aldrich).

Determination of the dissociation constants of UehA for ectoine and 5-hydroxyectoine

The UehA protein contains 14 tyrosine and 2 tryptophane residues, which allowed us to measure the binding of ectoine and 5-hydroxyectoine by the purified UehA protein through the use of an intrinsic tryptophan–tyrosine fluorescence-based binding assay.[24,31,32] Fluorescence spectroscopy measurements were performed using a Cary Eclipse fluorescence photometer (VARIAN, Palo Alto, CA). The excitation wavelength was set to 280 nm (slit width = 5 nm), and temperature was maintained at 25 ± 1 °C using a circulating water bath. A UehA protein solution (5 μg/ml in 10 mM Tris–HCl, pH 7.5, and 10 mM NaCl) was mixed with either ectoine or 5-hydroxyectoine solution (in 10 mM Tris–HCl, pH 7.5, and 10 mM NaCl). The mixture was then incubated for 2 min to allow equilibration before the actual measurement. Emission spectra were monitored from 280 to 410 nm using the program Cary Eclipse Scan (VARIAN). Upon substrate binding, a decrease in the fluorescence intensity of UehA was detected, and this change in the emission spectrum was used to determine the K_d values for the UehA protein for either ectoine or 5-hydroxyectoine by plotting the peak area from 295 to 400 nm against the substrate concentration. For convenience, data were converted into fluorescence increase and treated as and analyzed by assuming a standard one-site binding model according to:

$$F_{cor} = F_0 + (\Delta F[S_0]/[S_0] + K_d)$$

where F_{cor} is the fluorescence intensity for a given substrate concentration, F_0 is the fluorescence intensity without substrate, ΔF is the maximal change in fluorescence intensity, $[S_0]$ is the substrate concentration and K_d is the binding constant. For all concentrations, the total substrate concentration (bound and free substrates) was used in the calculations. All K_d measurements of UehA for its substrates ectoine and 5-hydroxyectoine represent the average of at least three independent measurements, with standard deviations.

Crystallization

Crystallization trials were carried out using the hanging-drop vapor-diffusion method at 18 °C. Homogenous UehA protein was concentrated to 12 mg ml^{-1} prior to crystallization. For crystallization of UehA with substrate, 2 mM ectoine was added to the protein solution 30 min prior to crystallization. Crystals were grown by mixing protein solution with a reservoir solution containing 100 mM Na–citrate, pH 5.6–6.0, and 2.4–2.6 M ammonium sulfate in a 1:1 ratio. Crystals normally grew in 5 to 10 days. Suitable crystals were cryoprotected using mother liquid supplemented with 30% (v/v) ethylene glycol and flash frozen in liquid nitrogen.

Data collection and structure determination

The ectoine dataset was collected at the ID23-2 beamline at the ESRF. Detailed information on data collection statistics are shown in Table 1. The optimal data collection strategy was calculated using the program BEST.[53] The collected dataset was processed with the DENZO[54] and XDS program packages. The TeaA model (kindly provided by Dr. C. Ziegler, Max-Planck-Institute of Biophysics, Frankfurt, Germany) was used as the template to phase the UehA dataset at 2.9 Å using the molecular replacement program PHASER[34] and further refined using REFMAC5[55] and COOT.[56] Dataset and refinement statistics are summarized in Table 1.

PDB accession code

Coordinates for the UehA–ectoine complex have been deposited in the PDB under accession code 3FXB.

Figure preparation

Figures of protein structures were prepared using PyMOL§.

Databank searches, sequence and structural alignments

Proteins that are homologous to the UehA, UehB, UehC and UspA proteins from *S. pomeroyi* DSS-3 were searched via the Web server of the DOE Joint Genome Institute‖ using the BLAST algorithm.[46] The genome context of finished and unfinished microbial genomes in the vicinity of the *uehA* gene was assessed using the gene neighborhood tool‖ provided by the JGI Web server. Sequence alignments of proteins were performed using ClustalW[47] as implemented in the Vector NTI 10.0 software package (Invitrogen, Karlsruhe, Germany). Predictions of signal

§ http://pymol.sourceforge.net/
‖ http://img.jgi.doe.gov/cgi-bin/pub/main.cgi

Please cite this article as: Lecher, J. *et al.*, The Crystal Structure of UehA in Complex with Ectoine—A Comparison with Other TRAP-T Binding Proteins, *J. Mol. Biol.* (2009), doi:10.1016/j.jmb.2009.03.077

sequences of secreted proteins were conducted using the SignalP 3.0 Web server¶.[57] The prediction of the topology of integral membrane proteins was performed with SCAMPI, which is part of the consensus topology prediction Web server TOPCONS[a].[30] Structure alignments were performed using LSQMAN employing standard settings.

Acknowledgements

This project was funded by grants from the University of Duesseldorf (L.S.), the University of Marburg, the Fonds der Chemischen Industrie and the Max-Planck-Institute for Terrestrial Microbiology (Marburg) (to E.B.). We are grateful to Dr. Christine Ziegler (Max-Planck-Institute of Biophysics, Frankfurt, Germany) for kindly providing us with the coordinates of the TehA crystal structure prior to publication. We are indebted to Margarete Schubert-Bätz for her excellent support in the early stages of the project and to Dr. Sacha Popov for his support during data collection at the ESRF beamline ID-23 (Grenoble, France) as well as Dr. Paul Tucker and Dr. Mathew Grooves at the BW7A beamline (EMBL Outstation Hamburg, Hamburg, Germany). We acknowledge support of in-house facilities by the NRW Research School BioStruct, and we also thank Dr. Thomas Schwarz from bitop AG (Witten, Germany) for the generous gift of ectoine and 5-hydroxyectoine and Dr. Mohamed Jebbar (University of Rennes, Rennes, France) for kindly providing us with radiolabeled ectoine.

Supplementary Data

Supplementary data associated with this article can be found, in the online version, at doi:10.1016/j.jmb.2009.03.077

References

1. Davidson, A. L., Dassa, E., Orelle, C. & Chen, J. (2008). Structure, function, and evolution of bacterial ATP-binding cassette systems. *Microbiol. Mol. Biol. Rev.* **72**, 317–364; table of contents.
2. Davidson, A. L. & Chen, J. (2004). ATP-binding cassette transporters in bacteria. *Annu. Rev. Biochem.* **73**, 241–268.
3. Orelle, C., Ayvaz, T., Everly, R. M., Klug, C. S. & Davidson, A. L. (2008). Both maltose-binding protein and ATP are required for nucleotide-binding domain closure in the intact maltose ABC transporter. *Proc. Natl Acad. Sci. USA*, **105**, 12837–12842.
4. Forward, J. A., Behrendt, M. C. & Kelly, D. J. (1993). Evidence that the high affinity C4-dicarboxylate transport system of *Rhodobacter capsulatus* is a novel type of periplasmic permease. *Biochem. Soc. Trans.* **21**, 343S.
5. Forward, J. A., Behrendt, M. C., Wyborn, N. R., Cross, R. & Kelly, D. J. (1997). TRAP transporters: a new family of periplasmic solute transport systems encoded by the dctPQM genes of *Rhodobacter capsulatus* and by homologs in diverse Gram-negative bacteria. *J. Bacteriol.* **179**, 5482–5493.
6. Kelly, D. J. & Thomas, G. H. (2001). The tripartite ATP-independent periplasmic (TRAP) transporters of bacteria and archaea. *FEMS Microbiol. Rev.* **25**, 405–424.
7. Rabus, R., Jack, D. L., Kelly, D. J. & Saier, M. H., Jr (1999). TRAP transporters: an ancient family of extracytoplasmic solute-receptor-dependent secondary active transporters. *Microbiology*, **145**(Pt 12), 3431–3445.
8. Mulligan, C., Kelly, D. J. & Thomas, G. H. (2007). Tripartite ATP-independent periplasmic transporters: application of a relational database for genome-wide analysis of transporter gene frequency and organization. *J. Mol. Microbiol. Biotechnol.* **12**, 218–226.
9. Mulligan, C., Geertsma, E. R., Severi, E., Kelly, D. J., Poolman, B. & Thomas, G. H. (2009). The substrate-binding protein imposes directionality on an electrochemical sodium gradient-driven TRAP transporter. *Proc. Natl Acad. Sci. USA*.
10. Shaw, J. G., Hamblin, M. J. & Kelly, D. J. (1991). Purification, characterization and nucleotide sequence of the periplasmic C4-dicarboxylate-binding protein (DctP) from *Rhodobacter capsulatus*. *Mol. Microbiol.* **5**, 3055–3062.
11. Walmsley, A. R., Shaw, J. G. & Kelly, D. J. (1992). The mechanism of ligand binding to the periplasmic C4-dicarboxylate binding protein (DctP) from *Rhodobacter capsulatus*. *J. Biol. Chem.* **267**, 8064–8072.
12. Johnston, J. W., Coussens, N. P., Allen, S., Houtman, J. C., Turner, K. H., Zaleski, A. *et al.* (2008). Characterization of the *N*-acetyl-5-neuraminic acid-binding site of the extracytoplasmic solute receptor (SiaP) of nontypeable *Haemophilus influenzae* strain 2019. *J. Biol. Chem.* **283**, 855–865.
13. Gonin, S., Arnoux, P., Pierru, B., Lavergne, J., Alonso, B., Sabaty, M. & Pignol, D. (2007). Crystal structures of an extracytoplasmic solute receptor from a TRAP transporter in its open and closed forms reveal a helix-swapped dimer requiring a cation for alpha-keto acid binding. *BMC Struct. Biol.* **7**, 11.
14. Rucktooa, P., Antoine, R., Herrou, J., Huvent, I., Locht, C., Jacob-Dubuisson, F. *et al.* (2007). Crystal structures of two *Bordetella pertussis* periplasmic receptors contribute to defining a novel pyroglutamic acid binding DctP subfamily. *J. Mol. Biol.* **370**, 93–106.
15. Kuhlmann, S. I., Terwisscha van Scheltinga, A. C., Bienert, R., Kunte, H. J. & Ziegler, C. (2008). 1.55 Å structure of the ectoine binding protein TeaA of the osmoregulated TRAP-transporter TeaABC from *Halomonas elongata*. *Biochemistry*, **47**, 9475–9485.
16. Cuneo, M. J., Changela, A., Miklos, A. E., Beese, L. S., Krueger, J. K. & Hellinga, H. W. (2008). Structural analysis of a periplasmic binding protein in the tripartite ATP-independent transporter family reveals a tetrameric assembly that may have a role in ligand transport. *J. Biol. Chem.* **283**, 32812–32820.
17. Muller, A., Severi, E., Mulligan, C., Watts, A. G., Kelly, D. J., Wilson, K. S. *et al.* (2006). Conservation of structure and mechanism in primary and secondary transporters exemplified by SiaP, a sialic acid binding virulence factor from *Haemophilus influenzae*. *J. Biol. Chem.* **281**, 22212–22222.
18. Wilkinson, J. & Verschueren, K. H. G. (2003). Crystal

¶ http://www.cbs.dtu.dk/services/SignalP/
[a] http://topcons.cbr.su.se/

structures of periplasmic solute-binding proteins in ABC transport complexes illuminate their function. In *ABC Proteins: From Bacteria to Man* (Holland, I. B., Cole, S. P. C., Kuchler, K. & Higgins, C. F., eds), pp. 187–208, Academic Press (Elsevier Science), London, UK.
19. Mao, B., Pear, M. R., McCammon, J. A. & Quiocho, F. A. (1982). Hinge-bending in L-arabinose-binding protein. The "Venus's-flytrap" model. *J. Biol. Chem.* **257**, 1131–1133.
20. Moran, M. A., Buchan, A., Gonzalez, J. M., Heidelberg, J. F., Whitman, W. B., Kiene, R. P. *et al.* (2004). Genome sequence of *Silicibacter pomeroyi* reveals adaptations to the marine environment. *Nature*, **432**, 910–913.
21. Brinkhoff, T., Giebel, H. A. & Simon, M. (2008). Diversity, ecology, and genomics of the *Roseobacter* clade: a short overview. *Arch. Microbiol.* **189**, 531–539.
22. Kempf, B. & Bremer, E. (1998). Uptake and synthesis of compatible solutes as microbial stress responses to high-osmolality environments. *Arch. Microbiol.* **170**, 319–330.
23. Grammann, K., Volke, A. & Kunte, H. J. (2002). New type of osmoregulated solute transporter identified in halophilic members of the bacteria domain: TRAP transporter TeaABC mediates uptake of ectoine and hydroxyectoine in *Halomonas elongata* DSM 2581$^{(T)}$. *J. Bacteriol.* **184**, 3078–3085.
24. Hanekop, N., Hoing, M., Sohn-Bosser, L., Jebbar, M., Schmitt, L. & Bremer, E. (2007). Crystal structure of the ligand-binding protein EhuB from *Sinorhizobium meliloti* reveals substrate recognition of the compatible solutes ectoine and hydroxyectoine. *J. Mol. Biol.* **374**, 1237–1250.
25. Kuhlmann, A. U., Bursy, J., Gimpel, S., Hoffmann, T. & Bremer, E. (2008). Synthesis of the compatible solute ectoine in *Virgibacillus pantothenticus* is triggered by high salinity and low growth temperature. *Appl. Environ. Microbiol.* **74**, 4560–4563.
26. Kuhlmann, A. U. & Bremer, E. (2002). Osmotically regulated synthesis of the compatible solute ectoine in *Bacillus pasteurii* and related *Bacillus* spp. *Appl. Environ. Microbiol.* **68**, 772–783.
27. Bursy, J., Pierik, A. J., Pica, N. & Bremer, E. (2007). Osmotically induced synthesis of the compatible solute hydroxyectoine is mediated by an evolutionarily conserved ectoine hydroxylase. *J. Biol. Chem.* **282**, 31147–31155.
28. Bursy, J., Kuhlmann, A. U., Pittelkow, M., Hartmann, H., Jebbar, M., Pierik, A. J. & Bremer, E. (2008). Synthesis and uptake of the compatible solutes ectoine and 5-hydroxyectoine by *Streptomyces coelicolor* A3(2) in response to salt and heat stress. *Appl. Environ. Microbiol.* **74**, 7286–7296.
29. Jebbar, M., Sohn-Bosser, L., Bremer, E., Bernard, T. & Blanco, C. (2005). Ectoine-induced proteins in *Sinorhizobium meliloti* include an ectoine ABC-type transporter involved in osmoprotection and ectoine catabolism. *J. Bacteriol.* **187**, 1293–1304.
30. Bernsel, A., Viklund, H., Falk, J., Lindahl, E., von Heijne, G. & Elofsson, A. (2008). Prediction of membrane-protein topology from first principles. *Proc. Natl Acad. Sci. USA*, **105**, 7177–7181.
31. Horn, C., Sohn-Bosser, L., Breed, J., Welte, W., Schmitt, L. & Bremer, E. (2006). Molecular determinants for substrate specificity of the ligand-binding protein OpuAC from *Bacillus subtilis* for the compatible solutes glycine betaine and proline betaine. *J. Mol. Biol.* **357**, 592–606.
32. Oswald, C., Smits, S. H., Hoing, M., Sohn-Bosser, L., Dupont, L., Le Rudulier, D. *et al.* (2008). Crystal structures of the choline/acetylcholine substrate binding protein ChoX from *Sinorhizobium meliloti* in the liganded and unliganded closed states. *J. Biol. Chem.* **283**, 32848–32859.
33. Kabsch, W. (1993). Automatic processing of rotation diffraction data from crystals of initially unknown symmetry and cell constants. *J. Appl. Crystallogr.* **26**, 795–800.
34. McCoy, A. J., Grosse-Kunstleve, R. W., Adams, P. D., Winn, M. D., Storoni, L. C. & Read, R. J. (2007). Phaser crystallographic software. *J. Appl. Crystallogr.* **40**, 658–674.
35. Fukami-Kobayashi, K., Tateno, Y. & Nishikawa, K. (1999). Domain dislocation: a change of core structure in periplasmic binding proteins in their evolutionary history. *J. Mol. Biol.* **286**, 279–290.
36. Street, T. O., Bolen, D. W. & Rose, G. D. (2006). A molecular mechanism for osmolyte-induced protein stability. *Proc. Natl Acad. Sci. USA*, **103**, 13997–14002.
37. Smits, S. H., Hoing, M., Lecher, J., Jebbar, M., Schmitt, L. & Bremer, E. (2008). The compatible solute-binding protein OpuAC from *Bacillus subtilis*: ligand-binding, site directed mutagenesis and crystallographic studies. *J. Bacteriol.* Q2
38. Schiefner, A., Holtmann, G., Diederichs, K., Welte, W. & Bremer, E. (2004). Structural basis for the binding of compatible solutes by ProX from the hyperthermophilic archaeon *Archaeoglobus fulgidus*. *J. Biol. Chem.* **279**, 48270–48281.
39. Schiefner, A., Breed, J., Bosser, L., Kneip, S., Gade, J., Holtmann, G. *et al.* (2004). Cation–pi interactions as determinants for binding of the compatible solutes glycine betaine and proline betaine by the periplasmic ligand-binding protein ProX from *Escherichia coli*. *J. Biol. Chem.* **279**, 5588–5596.
40. Mahmood, N. A., Biemans-Oldehinkel, E., Patzlaff, J. S., Schuurman-Wolters, G. K. & Poolman, B. (2006). Ion specificity and ionic strength dependence of the osmoregulatory ABC transporter OpuA. *J. Biol. Chem.* **281**, 29830–29839.
41. Ott, V., Koch, J., Spate, K., Morbach, S. & Kramer, R. (2008). Regulatory properties and interaction of the C- and N-terminal domains of BetP, an osmoregulated betaine transporter from *Corynebacterium glutamicum*. *Biochemistry*, **47**, 12208–12218.
42. Culham, D. E., Vernikovska, Y., Tschowri, N., Keates, R. A., Wood, J. M. & Boggs, J. M. (2008). Periplasmic loops of osmosensory transporter ProP in *Escherichia coli* are sensitive to osmolality. *Biochemistry*, **47**, 13584–13593.
43. Oldham, M. L., Khare, D., Quiocho, F. A., Davidson, A. L. & Chen, J. (2007). Crystal structure of a catalytic intermediate of the maltose transporter. *Nature*, **450**, 515–521.
44. Hollenstein, K., Frei, D. C. & Locher, K. P. (2007). Structure of an ABC transporter in complex with its binding protein. *Nature*, **446**, 213–216.
45. Hvorup, R. N., Goetz, B. A., Niederer, M., Holenstein, K., Perozo, E. & Locher, K. P. (2007). Asymmetry in the structure of the ABC transporter-binding protein complex BtuCD–BtuF. *Science*, **317**, 1387–1390.
46. Altschul, S. F., Madden, T. L., Schaffer, A. A., Zhang, J., Zhang, Z., Miller, W. & Lipman, D. J. (1997). Gapped BLAST and PSI-BLAST: a new generation of protein database search programs. *Nucleic Acids Res.* **25**, 3389–3402.
47. Thompson, J. D., Higgins, D. G. & Gibson, T. J. (1994). CLUSTAL W: improving the sensitivity of progressive

Please cite this article as: Lecher, J. *et al.*, The Crystal Structure of UehA in Complex with Ectoine—A Comparison with Other TRAP-T Binding Proteins, *J. Mol. Biol.* (2009), doi:10.1016/j.jmb.2009.03.077

multiple sequence alignment through sequence weighting, position-specific gap penalties and weight matrix choice. *Nucleic Acids Res.* **22**, 4673–4680.
48. Kvint, K., Nachin, L., Diez, A. & Nystrom, T. (2003). The bacterial universal stress protein: function and regulation. *Curr. Opin. Microbiol.* **6**, 140–145.
49. Jebbar, M., Talibart, R., Gloux, K., Bernard, T. & Blanco, C. (1992). Osmoprotection of *Escherichia coli* by ectoine: uptake and accumulation characteristics. *J. Bacteriol.* **174**, 5027–5035.
50. Gonzalez, J. M., Covert, J. S., Whitman, W. B., Henriksen, J. R., Mayer, F., Scharf, B. *et al.* (2003). *Silicibacter pomeroyi* sp. nov. and *Roseovarius nubinhibens* sp. nov., dimethylsulfoniopropionate-demethylating bacteria from marine environments. *Int. J. Syst. Evol. Microbiol.* **53**, 1261–1269.
51. Baumann, P., Baumann, L. & Mandel, M. (1971). Taxonomy of marine bacteria: the genus *Beneckea*. *J. Bacteriol.* **107**, 268–294.
52. Miller, J. H. (1992). *A Short Course in Bacterial Genetics. A Laboratory Manual and Handbook for Escherichia coli and Related Bacteria*, Cold Spring Harbor Laboratory, Cold Spring Harbor, NY.
53. Popov, A. N. & Bourenkov, G. P. (2003). Choice of data-collection parameters based on statistic modelling. *Acta Crystallogr., Sect. D: Biol. Crystallogr.* **59**, 1145–1153.
54. Otwinowski, Z. & Minor, W. (1997). Processing of X-ray diffraction data collected in oscillation mode. In *Methods Enzymology* (Carter, C. W. & Sweet, R. M., eds), Vol. 276, Academic Press, London, UK.
55. Murshudov, G., Vagin, A. A. & Dodson, E. J. (1997). Refinement of macromolecular structures by the maximum-likelihood method. *Acta Crystallogr., Sect. D: Biol. Crystallogr.* **53**, 240–255.
56. Emsley, P. & Cowtan, K. (2004). Coot: model-building tools for molecular graphics. *Acta Crystallogr., Sect. D: Biol. Crystallogr.* **60**, 2126–2132.
57. Bendtsen, J. D., Nielsen, H., von Heijne, G. & Brunak, S. (2004). Improved prediction of signal peptides: SignalP 3.0. *J. Mol. Biol.* **340**, 783–795.

Please cite this article as: Lecher, J. *et al.*, The Crystal Structure of UehA in Complex with Ectoine—A Comparison with Other TRAP-T Binding Proteins, *J. Mol. Biol.* (2009), doi:10.1016/j.jmb.2009.03.077